

# NASA CONTRACTOR REPORT

NASA CR - 61051

NASA CR - 61051

FACILITY FORM 602	N65-24016	
	(ACCESSION NUMBER)	(THRU)
	52	1
	(PAGES)	(CODE)
CR-61051	10	
(NASA CR OR TMX CR AD NUMBER)	(CATEGORY)	

## APOLLO EXTENSION SYSTEM LSV STUDIES

### REPORT ON

### MISSION COMMAND AND CONTROL

Prepared under Contract No. NAS8-11096 by

Arch W. Meagher and Robert J. Bonham

Space Systems Section  
 NORTHROP SPACE LABORATORIES  
 6025 Technology Drive,  
 Huntsville, Alabama

GPO PRICE \$ \_\_\_\_\_

OTS PRICE(S) \$ \_\_\_\_\_

Hard copy (HC) \$3.00

Microfiche (MF) .50

For

NASA - GEORGE C. MARSHALL SPACE FLIGHT CENTER  
 Huntsville, Alabama

April 19, 1965

CR-61051

APOLLO EXTENSION SYSTEM LSV STUDIES

REPORT ON

MISSION COMMAND AND CONTROL

By

Arch W. Meagher  
Robert J. Bonham

Distribution of this report is provided in the interest of information exchange. Responsibility for the contents resides in the author or organization that prepared it.

Prepared under Contract No. NAS 8-11096 by

SPACE SYSTEMS SECTION  
Northrop Space Laboratories  
6025 Technology Drive,  
Huntsville, Alabama

For

R-ASTR-A  
ASTRONICS LABORATORY

NASA - GEORGE C. MARSHALL SPACE FLIGHT CENTER

## PREFACE

This Technical Report was prepared by the Northrop Space Laboratories (NSL), Huntsville, Department, for the George C. Marshall Space Flight Center under authorization of Task Order N-61, Contract NAS8-11096.

The NASA Technical Representative was Mr. John F. Pavlick of the MSFC Astrionics Laboratory(R-ASTR-A).

The work was a twenty man week effort ending on April 19, 1965.

The data presented herein include conceptual studies of the command and control systems for the major elements of remote and manual control of the LSV four-wheel vehicle. Also included are preliminary servo-analysis studies of the steering complex, and a discussion of the human performance in the control loop. Two approaches to the steering discussion are considered - that of wheel-angle control and that of heading control.

Suspension performance and effects of terrain slope on the vehicle performance were studied and reported in an interim report under Task Order N-46, Contract NAS8-11096. The report which was dated January 8, 1965, carried the number NASA CR-61040. Portions of that report are used as a basis of study for this report.

## TABLE OF CONTENTS

	Page
Summary	1
1.0 Introduction	2
2.0 Steering Concepts	7
2.1 General	7
2.2 Human Response	8
2.3 Steering by Continuous Wheel Angle Control	11
2.4 Steering by Heading Control	24
3.0 Steering Synchronizing Concepts	28
4.0 Automatic Change of Vehicle Operating Limits	32
5.0 Conclusions and Recommendations	34
6.0 Symbols	35
References	36
7.0 Appendix	37

## ILLUSTRATIONS

<u>FIGURE</u>	<u>TITLE</u>	<u>PAGE</u>
1	Block Diagram for Study of LSV Steering Control	3
2	Servo Diagram for Continuous Wheel Angle Control	11
3	Root Locus for 1/30 hp System	12
4a	Root Locus for System A	14
4b	Root Locus for System A (Modified)	15
4c	Root Locus for System A (Modified)	16
5a	Root Locus for System B	17
5b	Root Locus for System B (Modified)	18
6a	Root Locus for System C	19
6b	Root Locus for System C (Modified)	20
7a	Continuous Wheel Angle Control Diagram with operator in the loop operation	23
7b	Continuous Wheel Angle Control Diagram with operator in the loop - Earth-to-Lunar Operation	23
8a	Heading Control Servo Diagram (Lunar Operated)	25
8b	Heading Control Servo Diagram (Earth-to-Lunar Operated)	25
9a	Heading Control Servo Diagram - Non Linear (Lunar Operated)	26
9b	Heading Control Servo Diagram-Non Linear (Earth to Lunar Operated)	26

ILLUSTRATIONS (Continued)

		<u>PAGE</u>
10a	Synchronizing Circuit-Control → One Wheel	29
10b	Synchronizing Circuits-Control of Two Wheels	29
11	Synchronized Ackermann, 4-Wheel, and Crab Steering - Earth-to-Lunar Control	30

TABLES

I	Minimum <del>μ</del> Required for Roll Plane Slopes	4
---	---	---

SUMMARY

24016

This study is primarily limited to concepts of steering and the circuits involved. Root locus plots are presented for a basic part of the control complex where the system can be linearized. In order to obtain the constants necessary to determine the transfer functions for the root locus study, a number of steering motors were reviewed. The results of this review is shown in the appendix.

Since the control of the LSV will depend to a large degree on the performance of the operator, research concerning experiments in this area are reported. The application of the results of the experiments to the LSV operator is discussed.

Synchronizing of the individually controlled wheels is discussed, and a conceptual design for synchronizing circuits is presented.

Limits of operation of the LSV vary with conditions of speed and terrain. Automatic control of these limits is discussed.

Author →

INTRODUCTION

This report will cover portions of the steering problems of a 4-Wheel Lunar Surface Vehicle (LSV) and concepts for the control circuit involved. This vehicle was described in detail in report number NASA CR - 61040 (Reference 1) and a partial list of specifications are as follows:

Total vehicle mass	202.36 slugs
Vehicle tire constant	600 pounds per foot
Roll plane inertia	5075 slug feet squared
Pitch plane inertia	8116 slug feet squared
Tread width	11.5 feet (3.51 meters)
Wheelbase	17.6 feet (5.37 meters)
Height, Center of Gravity	5.83 feet (1.78 meters)

Figure 1 will be used as the basis for this study.

One of the parameters that can be calculated for use in the study of vehicle performance on Earth is the  $\mu$  of the soil over which the vehicle travels. In Reference 1 and other studies concerning control of the LSV,  $\mu$  was taken as the independent variable so that the results can reflect its true value when this value is known. This procedure will be followed in this report.

Since a skidding vehicle cannot progress in a turn, it is necessary to know skid limits. These limits for the LSV were



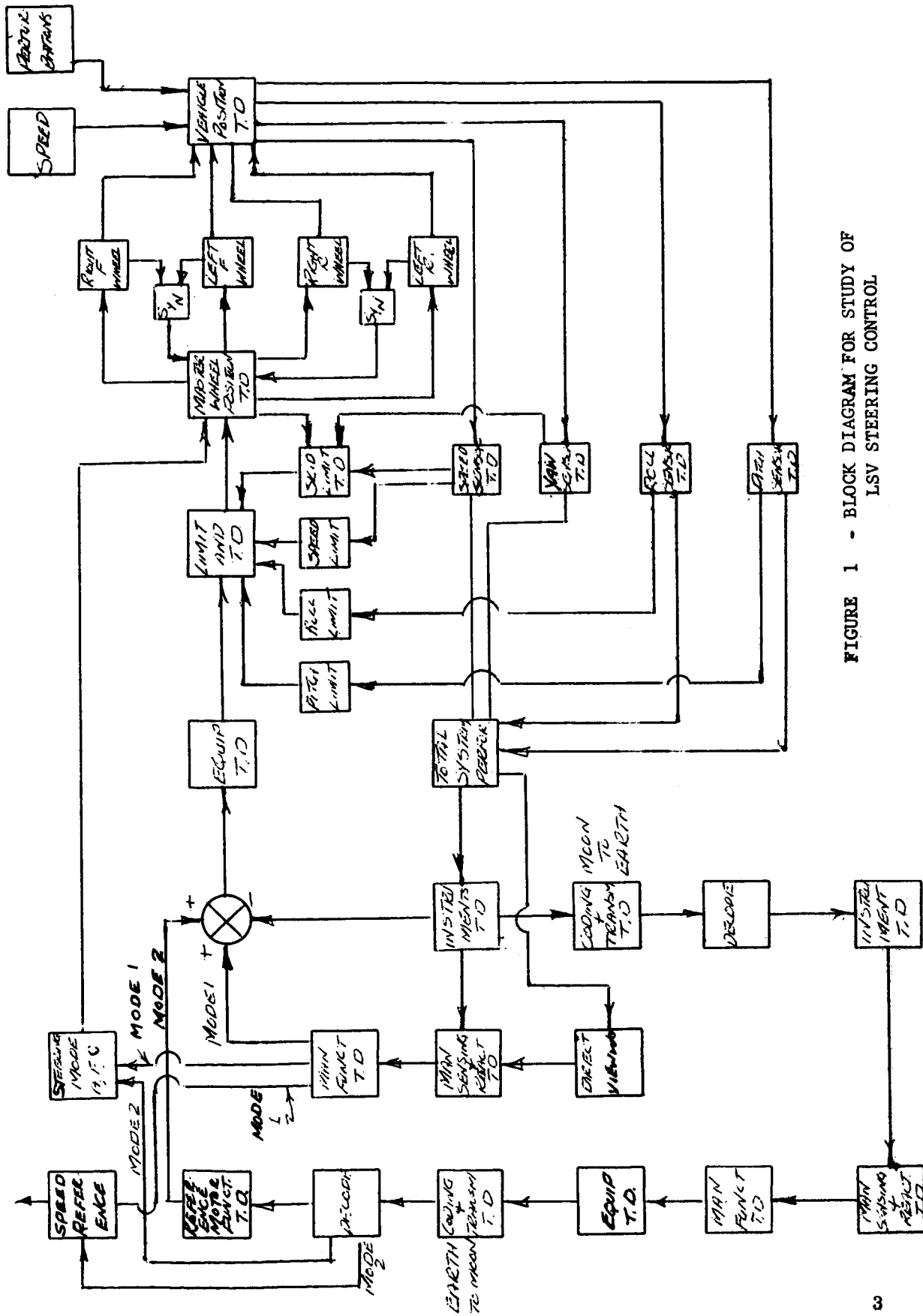


FIGURE 1 - BLOCK DIAGRAM FOR STUDY OF LSV STEERING CONTROL

TABLE I  
 Minimum Required for Roll Plane Slopes, Vehicle  
 Speed and Wheel Angle to Prevent Skidding  
 While Making an Up-slope Turn

Terrain Slope Degrees	Vehicle Speed, Km	Wheel Angle Degrees	Minimum $\mu$	Notes
0	8.36	12	0.2	
0	8.36	20	0.3	
0	16.72	4	0.2	
0	16.72	8	0.5	
0	16.72	12	1.0	-- Vehicle over-turn at 13-14° for $\mu = 1.0$
10	8.36	12	0.22	
10	8.36	20	0.33	
10	16.72	4	0.23	
10	16.72	8	0.6	
10	16.72	10	1.0	-- Vehicle overturn at 12-14° for $\mu = 1.0$
20	8.36	12	0.33	
20	8.36	20	0.45	
20	16.72	4	0.25	
20	16.72	8	0.8	-- Vehicle over-turn at 8-10° for $\mu = 1.0$
30	8.36	12	0.5	
30	8.36	20	0.65	
30	16.72	4	0.5	
30	16.72	6	0.7	--Vehicle over-turn at 6-7° for $\mu = 1.0$

established in Reference 1 and are repeated here for convenience in Table I. The  $\mu$  of the table is the minimum allowable for no skidding with the conditions listed. It should be noted that skidding represents a nonlinearity in the servo-analysis of steering and will be treated as such.

Besides skidding the  $\mu$  of the soil affects the torque required to turn the wheel of the vehicle. This, in turn affects the motor size, horsepower, gear ratio and motor speed. That is, the motor constants are unknown and the exact basis for determining them are unknown. This makes the servo-analysis difficult, since the choice of one of these factors will to a certain extent determine other factors of the study. There are two approaches to the solution of the problem. The first (and the preferred one) is the programming of an analog computer so that the steering is made to conform with the necessary performance determined from previous dynamic studies. The range of linear control and the effects of nonlinearities could be determined. From these results motor constants, and gear ratios for turning rates could be determined.

A second approach to the solution of the problem is presented in this report. The approach assumes a maximum  $\mu$  of 1.0 with the vehicle standing still as the worst case of torque requirements. Motor sizes of different types are studied to determine those that may be used to perform the task of steering for the worst case,

and to find the needed system constants for servo-analysis. These studies are shown in Appendix A. Many motor-gear combinations can be chosen to perform under particular Lunar conditions. Those studied are only samples to serve as guides when the time comes to determine hardware.

Other items which are studied in this report are the effect of human performance in the control of steering and wheel-angle control versus heading control. The human performance studies are limited primarily to a discussion and selection of transfer functions which are derived by actual experimentation (Reference 2). The application of the work done in a similar field and its adaptation to this problem is of interest. The functioning of the man at the controls is one of the major problems of stability for either manual or manual-remote control of the LSV. In connection with the human performance the wheel-angle control versus heading control is discussed in detail.

A final item of interest covered in this report is that of synchronizing the steering motors for the three or four types of steering - Ackermann, four-wheel, and crab. The fourth type of steering - scuff - requires no steering motors. Problems of steering synchronization are discussed with the presentation of a conceptual design.

## 2.0 STEERING CONCEPTS

### 2.1 General

The two steering control concepts; heading by continuous control of wheel angle and by setting a reference heading, each employ an electro-mechanical system. Each system may be used manually or remote-manually. The former is the simpler of the two from an equipment viewpoint, but it requires continuous reference changing to affect a change in heading. This steering mode can be compared to that of driving an automobile. The servo diagram is shown in Figure 2 of Section 2.3.

The second concept of steering is accomplished by setting a reference heading and having the vehicle accomplish the change automatically through a servo system employing the directional gyro as a feedback. This system consists of an inner loop control of the wheel angle and the outer loop employing the gyro. Continuous monitoring by the vehicle operator must be done to avoid obstacles through an override feature. The system is less stable than the simple system using wheel angle control only. It does, however, require less effort on the part of the operator. A servo diagram of this system is shown in Figure 9 of Section 2.4.

Both systems may be used with digital control (step-type) systems or with analog (ramp-type) systems. The difference in manual and remote-manual operation can be minimized to that of the time delay represented in radio transmission - by proper implementation. The time, while negligible on the Lunar surface, is approximately 3.0 seconds for the manual-remote operation from Earth.

The human operator may be described as an adaptive optimizing servo element. That is he will adjust his response to give the over all system the type of response which the operator desires. The operator is limited in his ability to adapt by his training and physical and mental response time. In attempting to develop a transfer function to describe a human operator it has been found that the general equation which fits well for this situation (Reference 2) is as follows:

$$\frac{K_p e^{-Ts}}{(T_1 s + 1)(T_n s + 1)} = G$$

The term  $e^{-Ts}$  represents the operator response time.

The value of T is dependent upon type of controls and the system response and varies from .12 to .2 seconds.

The term  $T_n$  comprises the effects of Neuromuscular lag and is partially adjustable for task.  $(T_L s + 1) / (T_1 s + 1)$  is considered to be the equalization term which adjusts to a particular forcing function and system.  $K_p$  is the operator gain which adjusts within limits for system stability. The operators mental attitude affects the value of  $K_p$  with strong motivation increasing its value. In addition there are nonlinear aspects to an operators performance which are more pronounced when high frequency forcing functions are used.

Equations 1 through 5 show the effect of the control element on the transfer function of the operator. (These equations were derived in Reference 2).

CONTROLLED  
ELEMENT

FORCING  
FUNCTION

HUMAN OPERATOR  
DESCRIBING FUNCTION

Eq. 1.

$$\frac{1}{S/2 + 1}$$

Superimposed  
Sinusoids

$$\begin{aligned}w_1 &= .66 \text{ rad/sec} \\w_2 &= 1.68 \text{ rad/sec} \\w_3 &= 2.87 \text{ rad/sec} \\w_4 &= 4.27 \text{ rad/sec}\end{aligned}$$

$$\frac{8 e^{-.15s} (S/.9 + 1)}{(S/.15 + 1) (S/25 + 1)}$$

Eq. 2

$$\frac{1}{S}$$

Superimposed  
Sinusoids

$$\begin{aligned}w_1 &= .66 \text{ rad/sec} \\w_2 &= 1.68 \text{ rad/sec} \\w_3 &= 2.87 \text{ rad/sec} \\w_4 &= 4.27 \text{ rad/sec}\end{aligned}$$

$$\frac{3e^{-.15s} (S/.35 + 1)}{(S/.2 + 1)}$$

Eq. 3.

$$\frac{15}{S/2 + 1}$$

Random Noise  
Corner Frequency  
1 rad/sec

$$\frac{4 e^{-.2s} (S/.4 + 1)}{(S/.1 + 1)}$$

Eq. 4.

$$\frac{5}{S}$$

Random Noise  
Corner Frequency  
1 rad/sec

$$\frac{1 e^{-.2s} (S/.3 + 1)}{(S/.07 + 1)}$$

Eq. 5

$$\frac{1}{S}$$

Random Noise  
Corner Frequency  
1 rad/sec

$$\frac{3 e^{-.2s} (S/.3+1)}{(S/.07 + 1)}$$

When time delays are introduced into a system as in the transmission time delay in Earth Moon communication, the operator will attempt to adapt and compensate to maintain system stability to the limits of his ability.

When lags are first inserted into the loop the operator tends to overshoot until he acquires some experience with the new system response. An over all reduction in system gain is inserted by the operator. As the lag nears 2 seconds the system appears to the operator to have the response of a pure integrator( $K/S$ ). The operator transfer function for this type of system is shown in equations 2, 4 and 5.

The effect of changes in system gain on operator response can be seen in equations 4 and 5. As the control element gain goes from 1 to 5 the operator gain adjusts from 3 to 1 which tends to maintain a constant over all loop gain.

Equation one has been selected for use in this study for describing the operator response during local control of the vehicle. Equation 2 has been chosen to selected for describing the operator response for remote control of the vehicle from Earth.



## 2.3

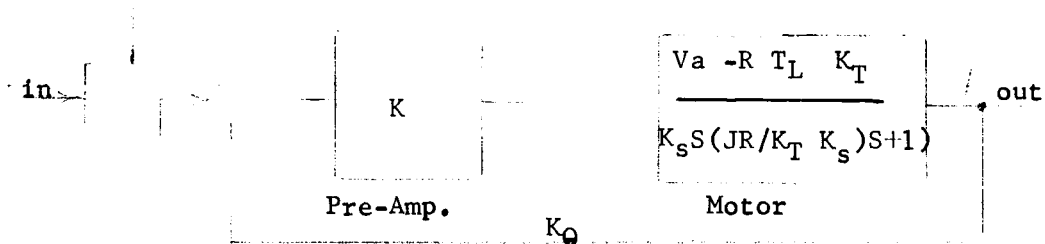
STEERING BY CONTINUOUS WHEEL ANGLE CONTROLDirectional  
Control \*

Figure 2 Servo Diagram for Continuous Wheel Angle Control.

The servo diagram of Figure 2 shows the feedback circuit for a shunt motor with a separately excited field, the transfer function for the motor-gear complex and the preamplifier. The  $\theta$  in is the position reference for the wheel angle and the  $\theta$  out is the actual wheel angle position. Other symbols are noted as follows:

- $K$  amplifier gain
- $V_a$  applied motor armature voltage, dc
- $R$  motor armature resistance, ohms
- $T_L$  steady-state load torque, ounce-inches
- $K_t$  motor torque constant, ounce-inches/ampere
- $K_s$  motor speed torque, volt-second/radian
- $J$  system inertia, ounce-inches squared
- $\frac{JR}{K_t K_s}$  system time constant, seconds
- $K_0$  voltage feedback per radian turn of motor

Polarities are reversed when the vehicle travel is reversed.

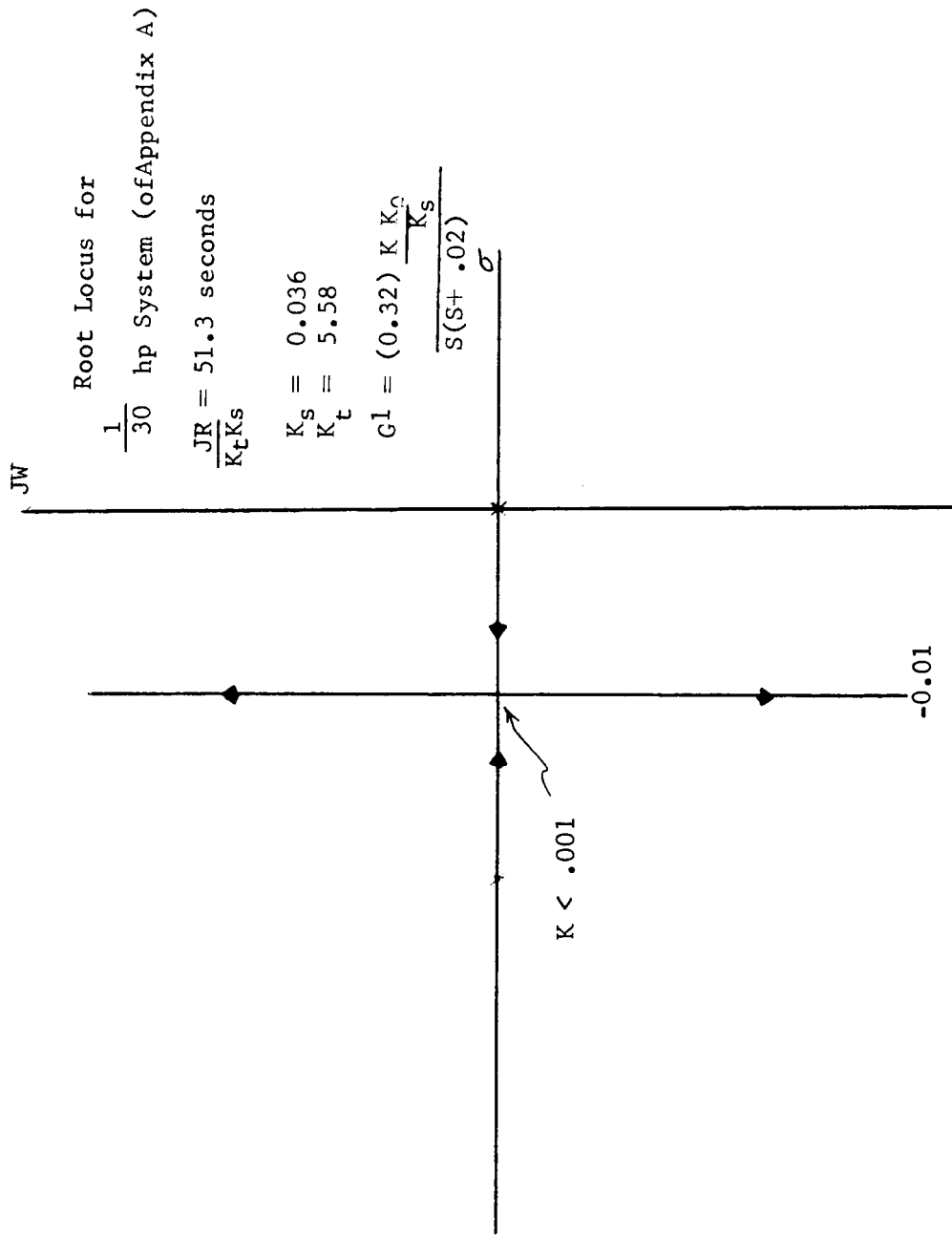


Figure 3

Using the system of Figure 2 the root locus plot was derived as shown in Figure 3, for the 1/30 Hp control type motor. The values of the constants were derived from the quantities in Appendix A. Root locus plots for the  $\frac{1}{16}$  Hp and  $\frac{1}{10}$  Hp motors are quite similar.

The root locus indicates that the system described will be stable (and oscillatory) but totally unsuited for the application. Primarily the fault lies with the values of  $K_s$  and  $K_t$ . While attempts could be made to add lead compensation to the circuits, it is felt that other systems could be used more advantageously. Accordingly, the 1/8 horsepower systems of Appendix A were calculated. The root locus for these systems are shown in Figures 4A, 4B and 4C.

Since the reference input voltage must be related to the  $K$ ,  $K_\theta$  and  $K_s$  of the system in a fashion determined by the hardware, the ratios of these constants are determined as a single value and recorded on the root locus plots. The reader can determine the voltage constant representing a specific value of  $\frac{K K_\theta}{K_s}$  in desired for motor starting across a 28 volt line and use this information to determine the value of  $K_\theta$  needed. In each case where a new reference is made digitally the system will respond as though a step were inserted, and it is from this viewpoint that the systems will be analyzed.

The root locus for SYSTEM A (derived in Appendix A) shows that this system for a wheel angle change of  $3^\circ$  per second will perform the change within the allotted time for a combination of  $\frac{K K_\theta}{K_s}$  equal to

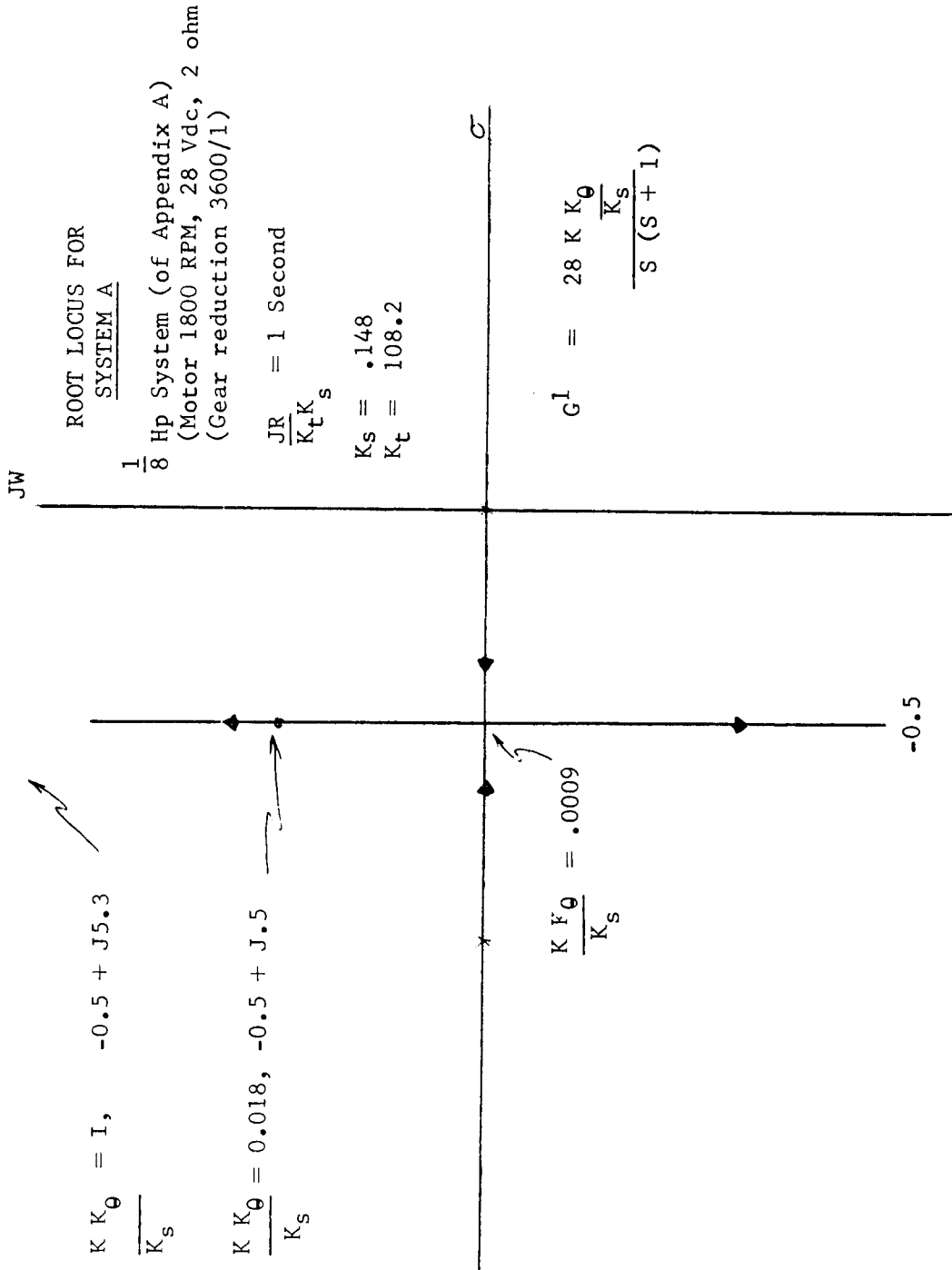
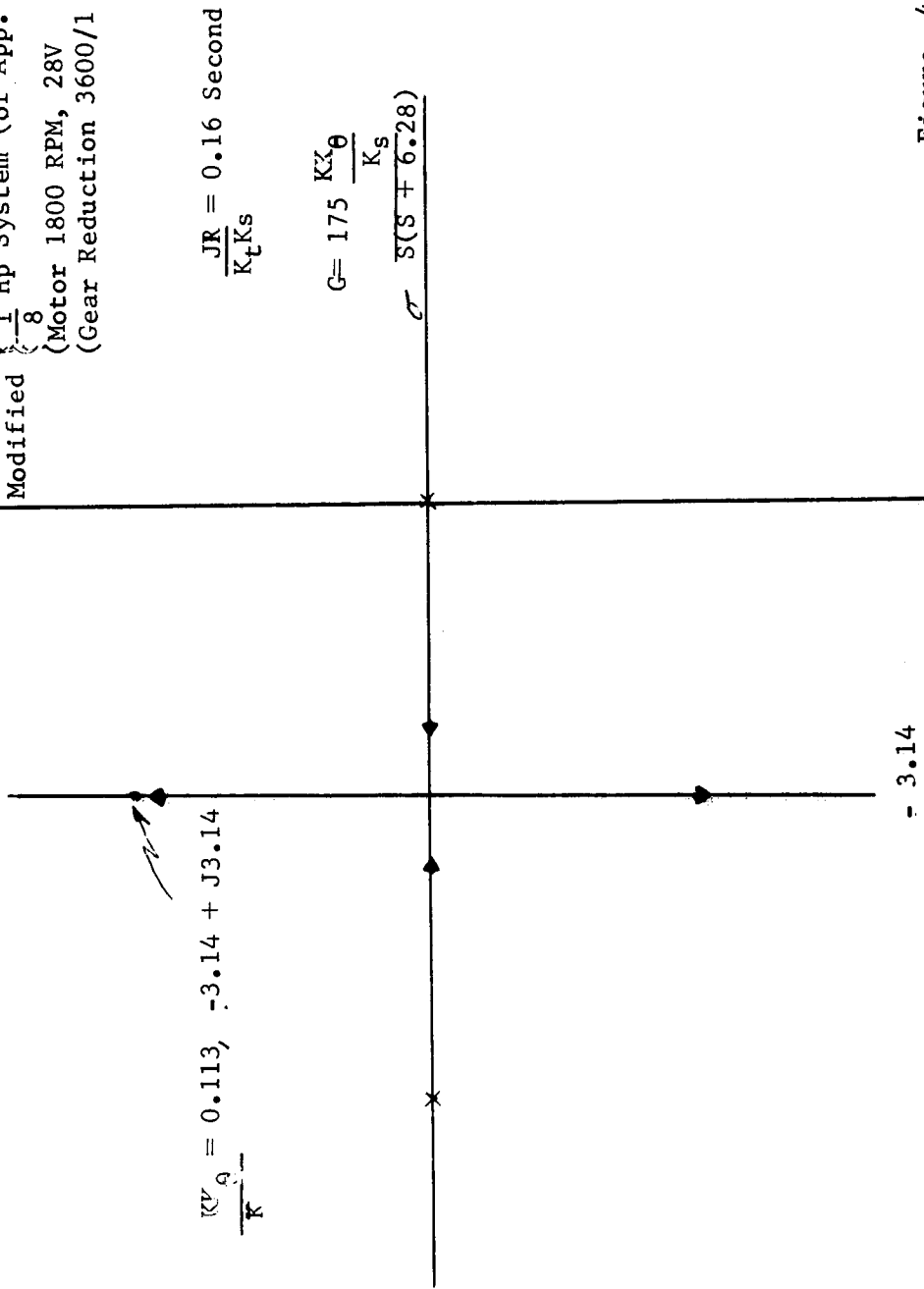


Figure 4A

ROOT LOCUS FOR  
 SYSTEM A (Modified)  
 Modified  $\left\{ \frac{1}{8} \right.$  Hp System (of App. A)  
 (Motor 1800 RPM, 28V  
 (Gear Reduction 3600/1



- 3.14

Figure 4 B

ROOT LOCUS SKETCHES  
 (Modified  $\frac{1}{8}$  Hp System of Appendix A - 1800 RPM Motor)  
 SYSTEM A (Modified)

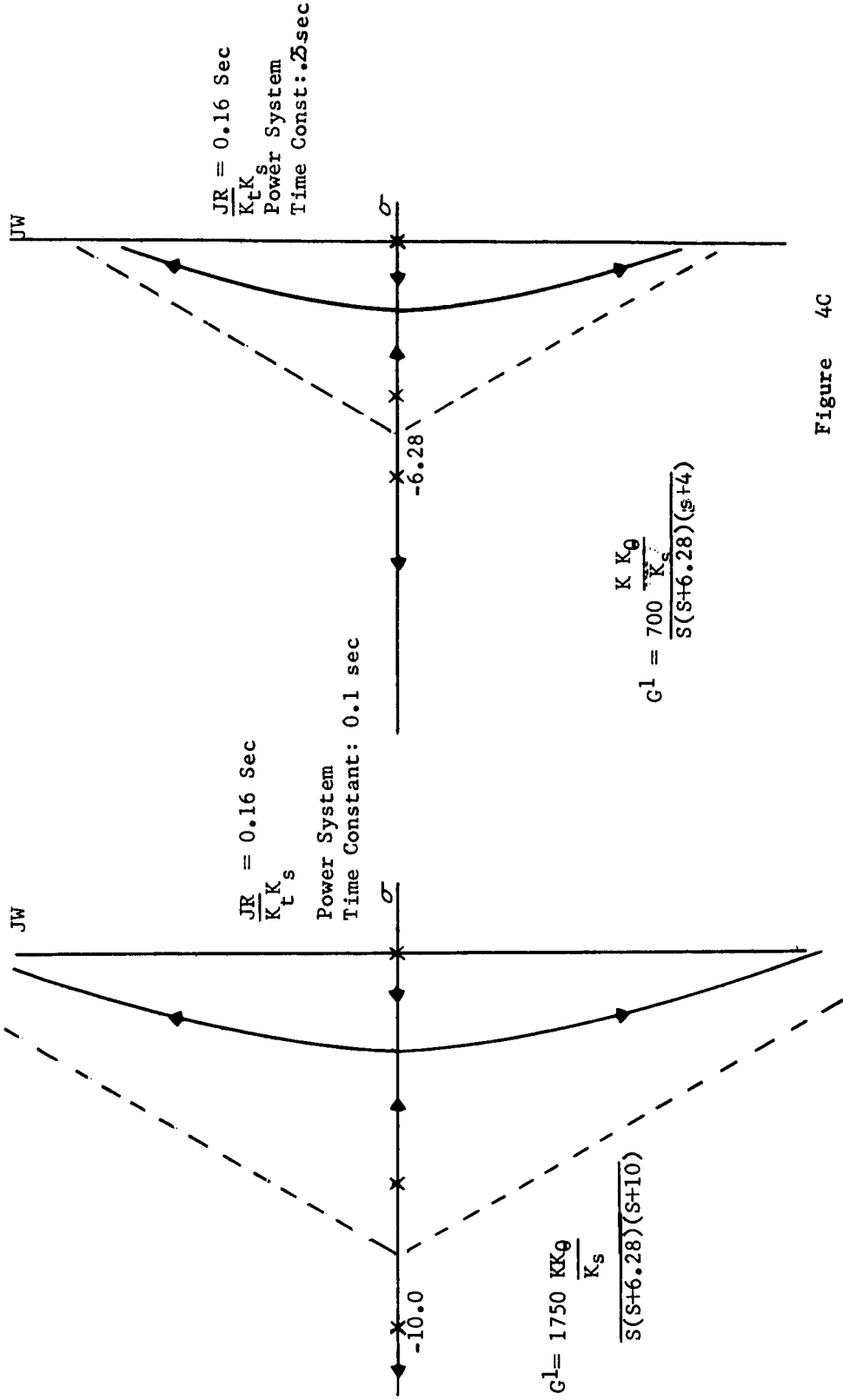


Figure 4C

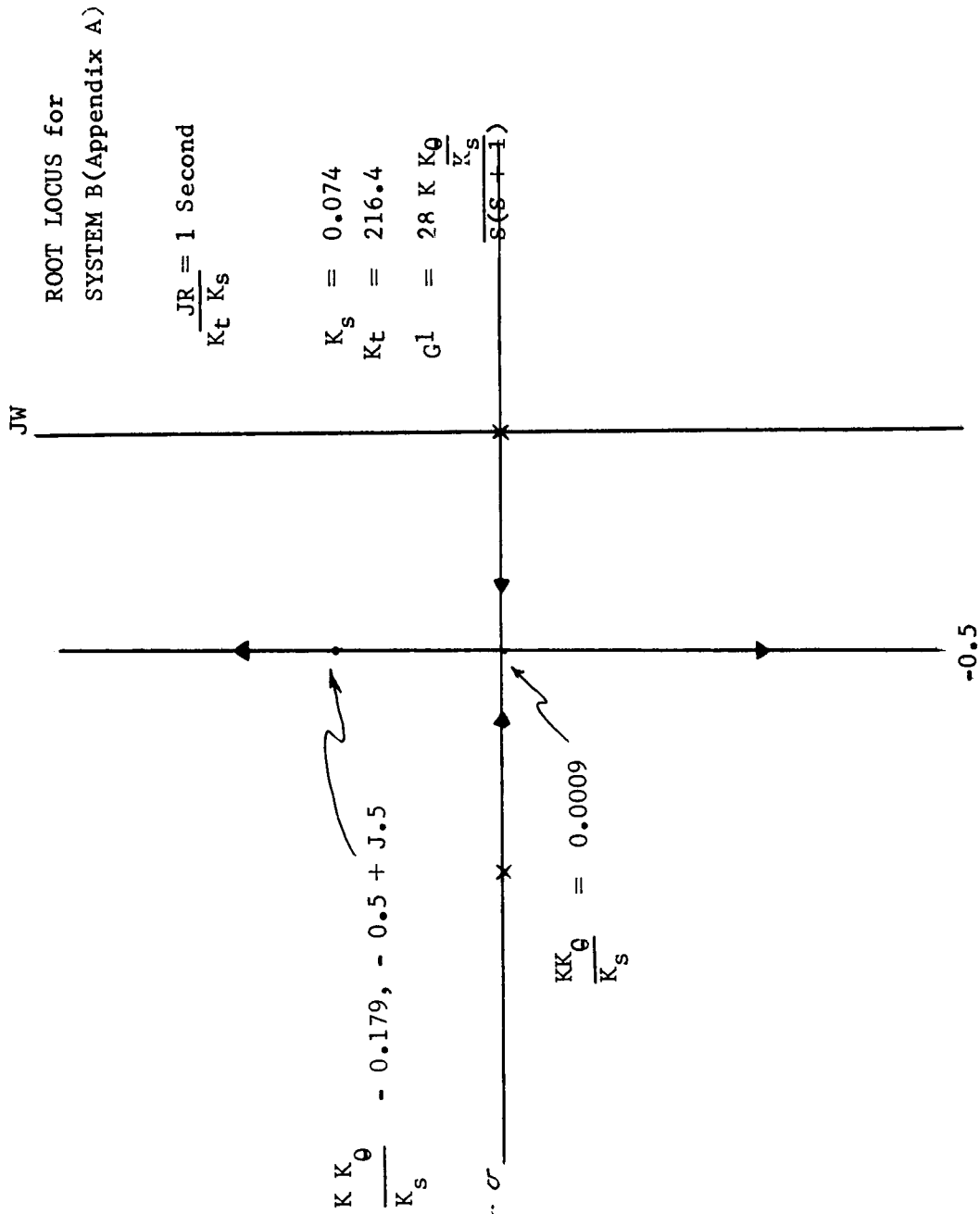


Figure 5 A

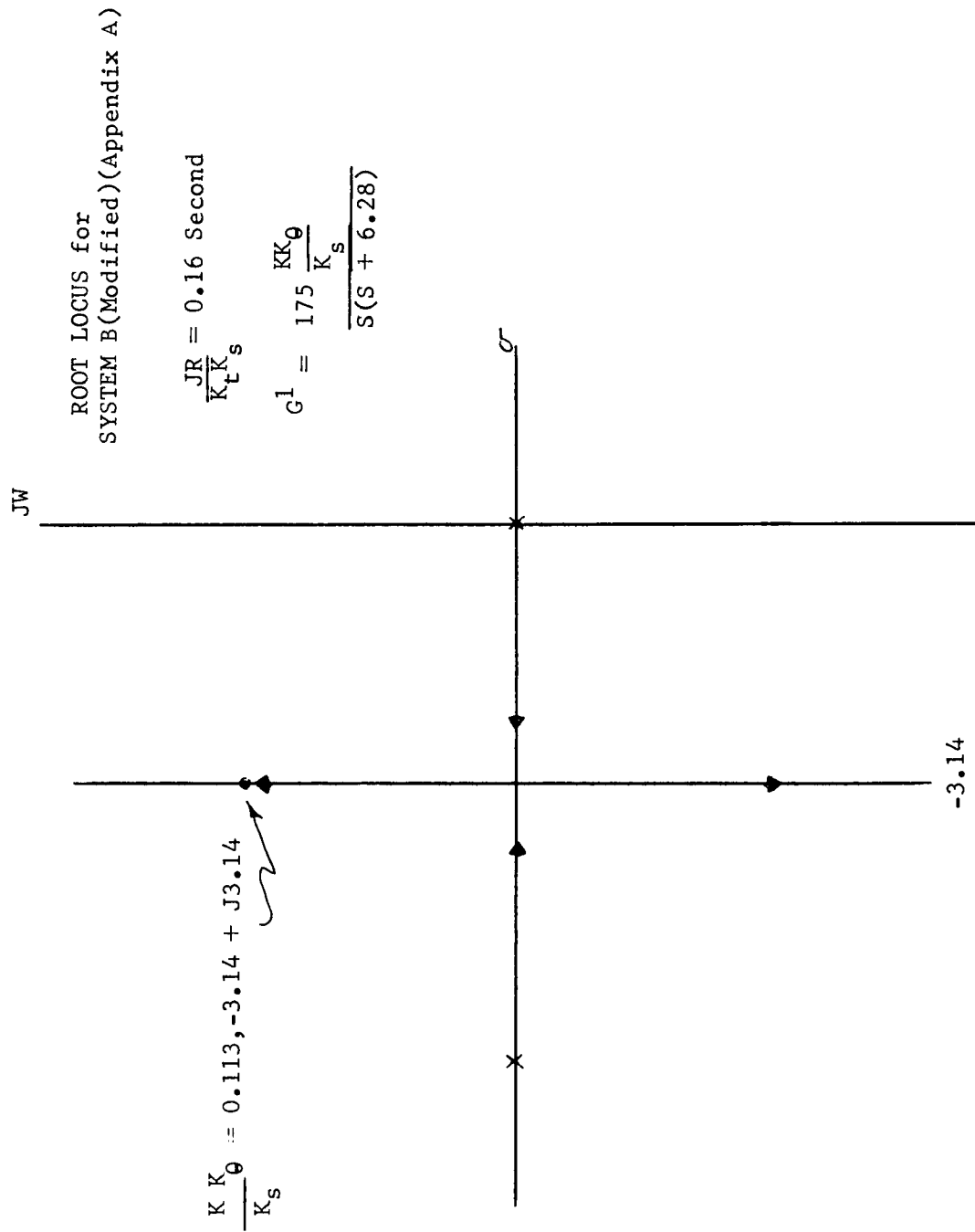


Figure 5 B



ROOT LOCUS FOR  
SYSTEM C (Appendix A)

JW

$$K K_0 = .226, \quad -.84 + j3.14$$

$$K K_0 = .03, \quad -.84 + j.84$$

$$\frac{JR}{K_t K_s} = .594 \text{ Second}$$

$$K_s = 0.129$$

$$K_t = 209$$

$$G_1 = \frac{47 K K_0}{S(S+1.68)}$$

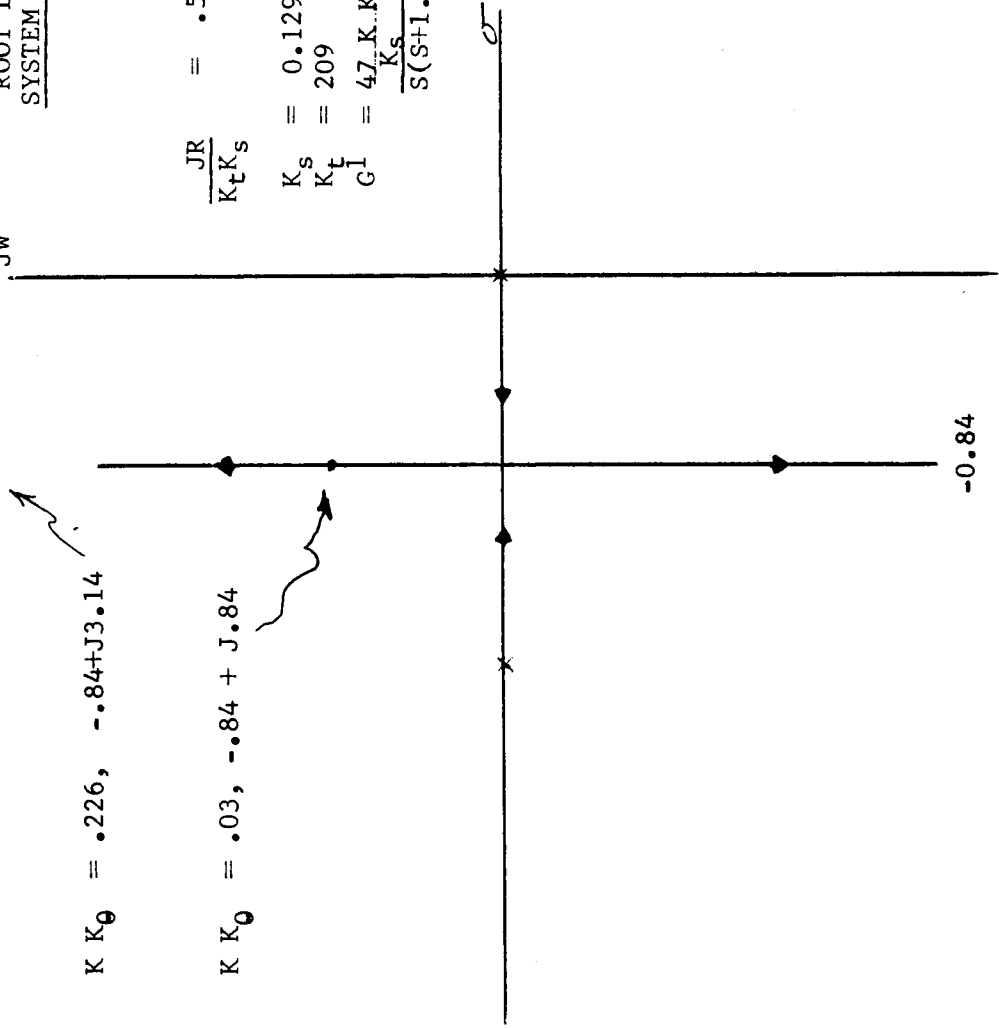


Figure 6 A

Root Locus for  
System C (Modified)(Appendix A)

$$\frac{JK}{K_t K_s} = 0.16 \text{ Second}$$

$$G^1 = 175 K \frac{K_\theta}{K_s} \frac{1}{S(S + 6.28)}$$

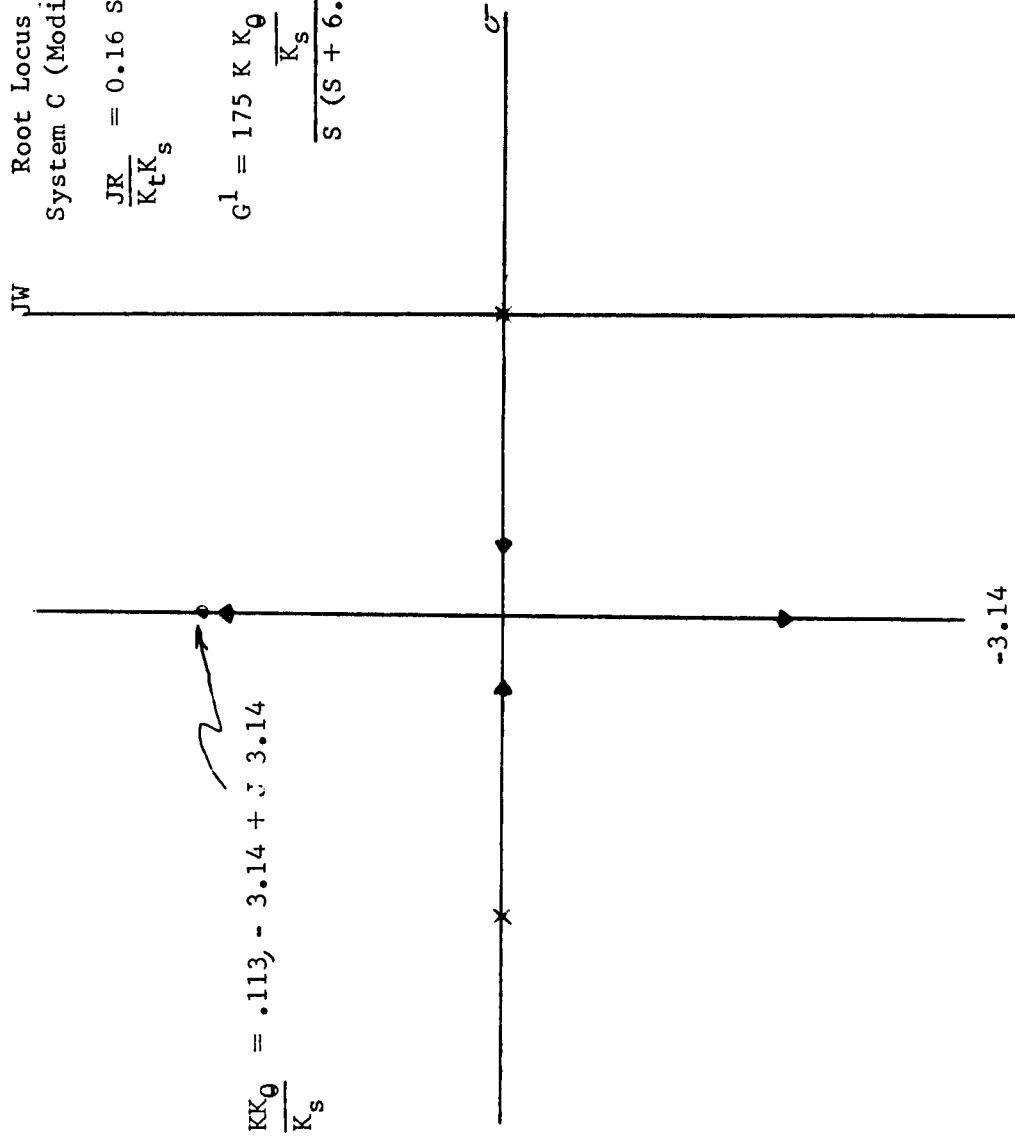


Figure 6 B

approximately 0.15. The system is oscillatory, however, and  $\zeta$  is approximately 0.2. Undoubtedly the system can be compensated (There are many combinations of compensation that will work) to achieve the desired performance. A better way for initial design, would be to lower the motor time constant by changing some elements of  $\frac{JR}{K_s K_t}$ . This was done for this system as shown in Figure 4B, and with a motor time constant of 0.16 second the specifications of having the wheel angle change  $3^\circ$  in one second are met with a gain combination (combination of the K's) of 0.113. The system now has a  $\zeta$  of approximately 0.7 which should be acceptable.

So far, in the analysis the time lag of the power supply has not been taken into consideration. If this is a factor to be considered, it can be analyzed by using  $\frac{K}{T_m s + 1}$  instead of K for the preamplifier. Root locus sketches showing power supply time lags of 0.1 and 0.25 second are shown in Figure 4C. It should be noted that lead compensation will be needed to balance any appreciable time lag in the power supply if the original specifications are to be met.

SYSTEMS B and C were derived in Appendix A for changes of wheel angle of  $6^\circ$  and  $9^\circ$  per second, respectively. The root locus plots of Figures 5 & 6 indicate that the specifications can be met also with K combinations of 0.113 and motor time constants of 0.16 second.

In making the above analysis it has been assumed that reference inputs for the systems have been limited to  $3^\circ$ ,  $6^\circ$  and  $9^\circ$  respectively. After the K combinations have been set by the hardware,

additional wheel angle changes (for instance, changing a  $6^\circ$  on the  $3^\circ$  system) will cause the system to reach the nonlinear region of operation. Since there is more than one nonlinearity present in the circuit, proper analysis will require an analog computer.

It should be remembered also that in making the above analysis the  $\mu$  of the soil was taken as 1.0, as the worst case. The  $\mu$  of the soil should not affect the results of SYSTEMS A, B, or C, however, since the motors used for the systems were separately excited shunt motors with nearly constant speeds. The variations in  $\mu$  will change the power output required from the motor but should not change the basic servo analysis. Conditions of  $\mu$  will change the effect (position limiting) of the heading on level ground or on slopes but not the wheel angle control.

Figures 7A and 7B show the transfer function block diagrams with the operator in the loop. The reasons for the choice of transfer functions were given in Section 2.2. For the case of Lunar operation, the operator observes continuously varying analog functions as the vehicle is steered. This is very similar to the conditions of the experiment that derived the operator transfer function used here for the Lunar operation. It was stated in Section 2.2 that for a time delay of over 2 seconds the control functions of equipment appear to the operator as an integral. The time delay for the Earth-to-Lunar operation is in excess of this, and the transfer shown appears to fit for this case. The time delay for transmission and equipment for transmission was taken as 3.0 seconds. It is included in the "operator" transfer function. Here, again, the system is considered to be in the linear range of operation.

CONTINUOUS WHEEL ANGLE CONTROL DIAGRAM  
WITH VEHICLE OPERATOR IN THE LOOP

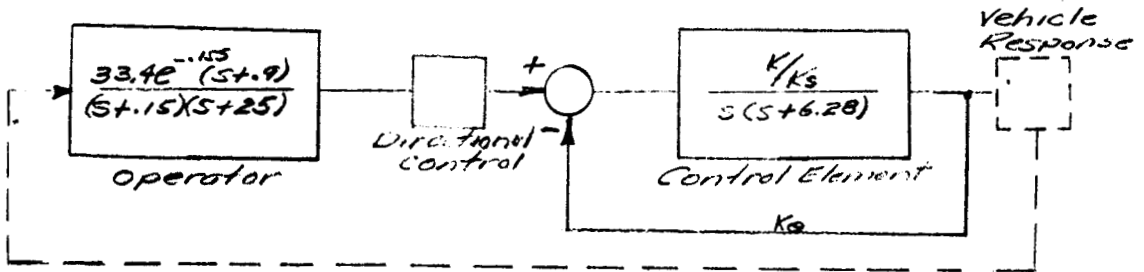


FIGURE 7A LUNAR OPERATION

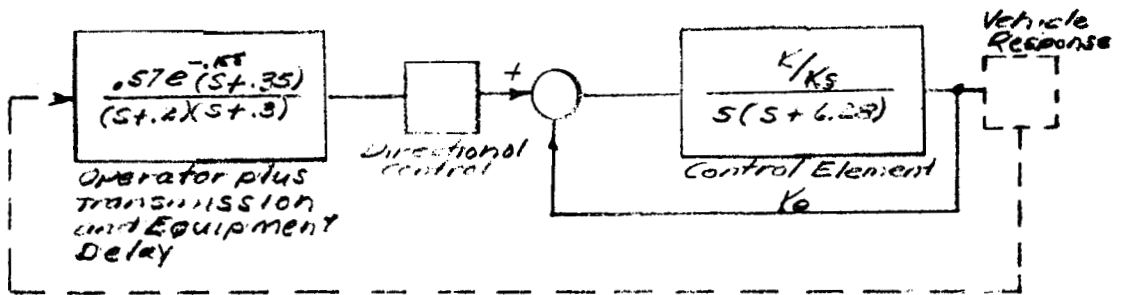


FIGURE 7B EARTH-TO-LUNAR OPERATION

## 2.4 Steering by Heading Control

The concept of steering by heading control is described as follows. The system operates in a fashion similar in many details to that of an automatic pilot. The operator sets the desired direction of travel as an input reference, and the control equipment on the vehicle, through the gyro feed back, automatically brings the vehicle to the new heading. This type of control has the distinct advantage of requiring less of the operator's time, and at the same time, reduces the effects of the transmission time delay for the Earth-to-Lunar mode of operation. There must be an override feature with the quipment for either the Lunar or the Earth-to-Lunar operation. This is used to avoid obstacles in the path of the set heading of the LSV.

Figures 8A & 8B show a simplified servo diagram of the heading control. The stability for this type of system is somewhat critical. The stability depends largely on power supply time lags, the gyro feed-back and particularly on the system gains. Turning rates could fall in the latter category as well as the other system constants (K's) described in Section 2.3. Note that the transmission time delays are included with the transfer function of the operator for the Earth-to-Lunar mode shown in Figure 8B. Power supply time delays are not shown.

Figures 9A and 9B show a block diagram of the two steering modes discussed with the nonlinearities involved. The descriptions of the systems are the same otherwise. These nonlinearities are physical limits of the vehicle's performance and must be included in any complete

HEADING CONTROL SERVO DIAGRAMS

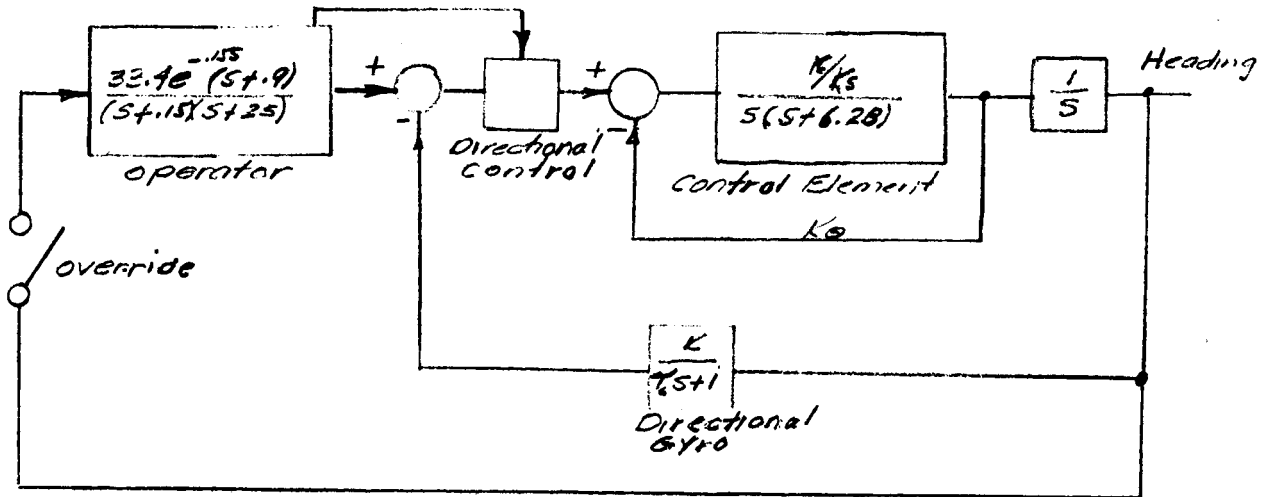


FIGURE 8A LUNAR OPERATION (LINEARIZED)

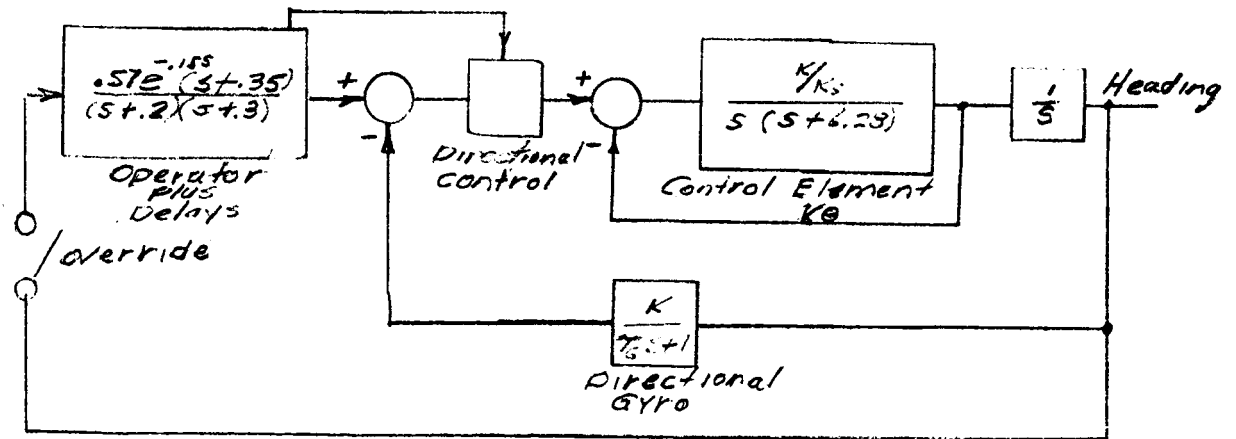


FIGURE 8B EARTH-TO-LUNAR OPERATION (LINEARIZED)

HEADING CONTROL - BLOCK DIAGRAM WITH NONLINEARITIES

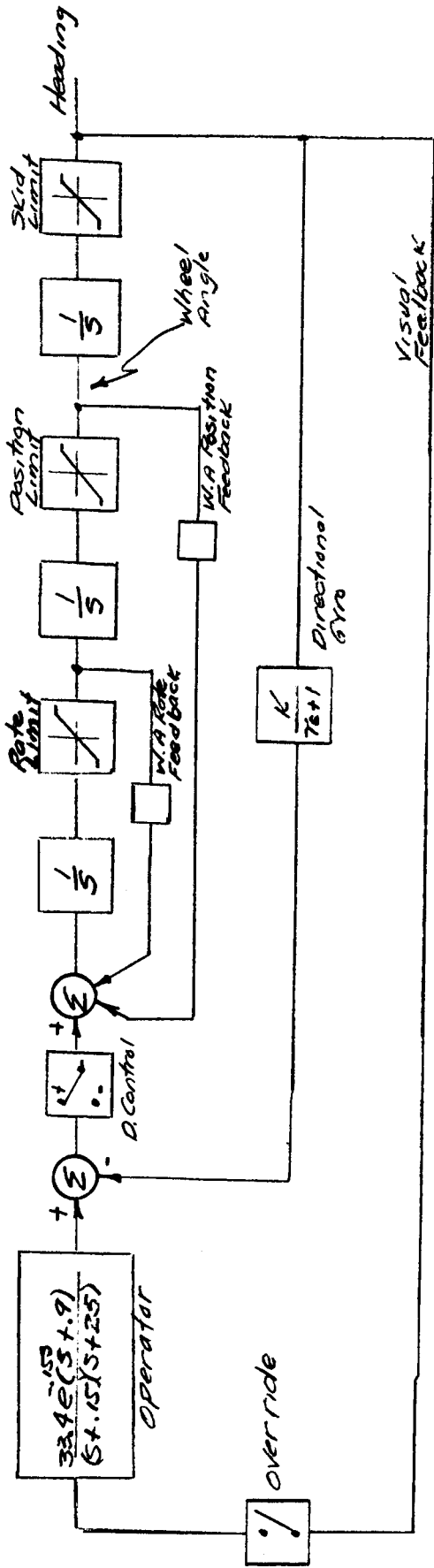


FIGURE 9A LUNAR OPERATION

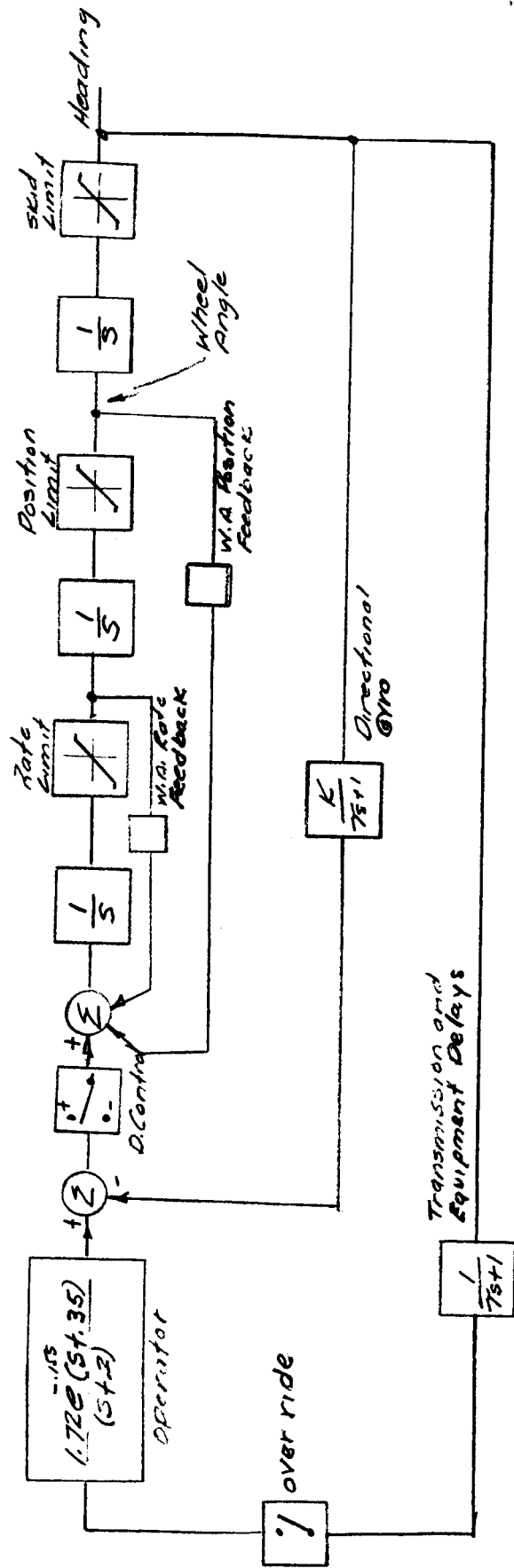


FIGURE 9B EARTH-TO-LUNAR OPERATION



analysis of the control system. The rate limit is determined by the top speed of the steering motor-gear combination; the position limit is determined by the total allowable (physical stop) wheel angle; and the skid limit occurs when the  $\mu$  of the soil does not support the vehicle's turning at the rate indicated by the wheel angle and vehicle's speed. This is the most troublesome of the limits on the steering. It is shown as a sat function to represent a full skid. Actually it has a variable amplitude and can be represented as a soft limit for a partial skid and represented as a hard limit for a full skid. Since the loss of steering when the LSV traverses a Lunar obstacle reacts in the same way as full or partial skidding, these functions also can be used to determine effects on steering when the LSV is partially (or fully) off of the Moon.

Concepts only are shown for this portion of the study. While some systems may be linearized and studied by servo analysis, more than one nonlinearity usually requires a computer for solutions.

Normally, little thought is given to the synchronizing of the wheels for steering of an earth-bound vehicle. This is done with a tie rod, and the steering is actuated from a common mechanical source. Concepts of the steering of the LSV, however, have indicated that each wheel will be actuated by individual electric motors - or that the design will not include a mechanical connection between the wheels to be steered. Therefore, a synchronizing device will be required for each pair of wheels used for steering. Figure 10 B shows a concept of such a synchronizing device. For this concept there is no master-slave relation between the prime movers of the wheels being steered. Instead, the prime mover with the largest output serves as master momentarily until the units are synchronized. As shown in Figure 10B, a small deadband should be inserted in the circuit for positive stability. While this circuit was conceived for use with electric motors, it should operate equally well in a hydraulic or pneumatic system if it is properly implemented.

The servo concepts for steering the LSV were studied in Sections 2.3 and 2.4 as though only one wheel of the vehicle is to be steered. This is adequate to determine the performance of the vehicle since the input constants can be doubled and the output constants halved for the pair of steered wheels, so that the previous work will apply. Figure 11 indicates a concept where three types of steering - Ackermann, 4-wheel and crab - can be used, and have these servo-analyses apply.

SYNCHRONIZING CIRCUITS

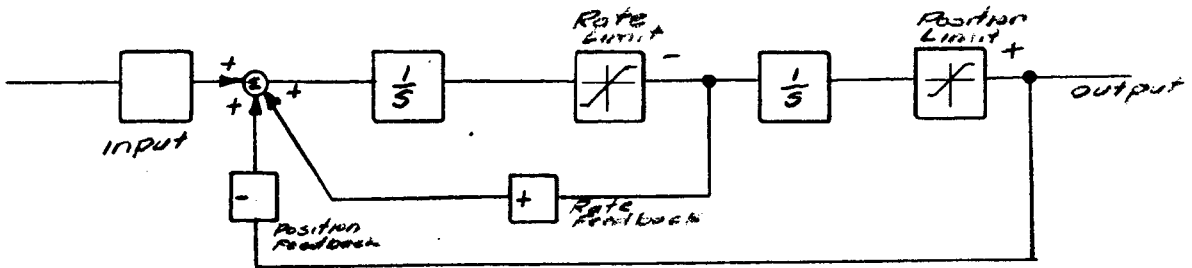


FIGURE 10A CONTROL OF ONE WHEEL

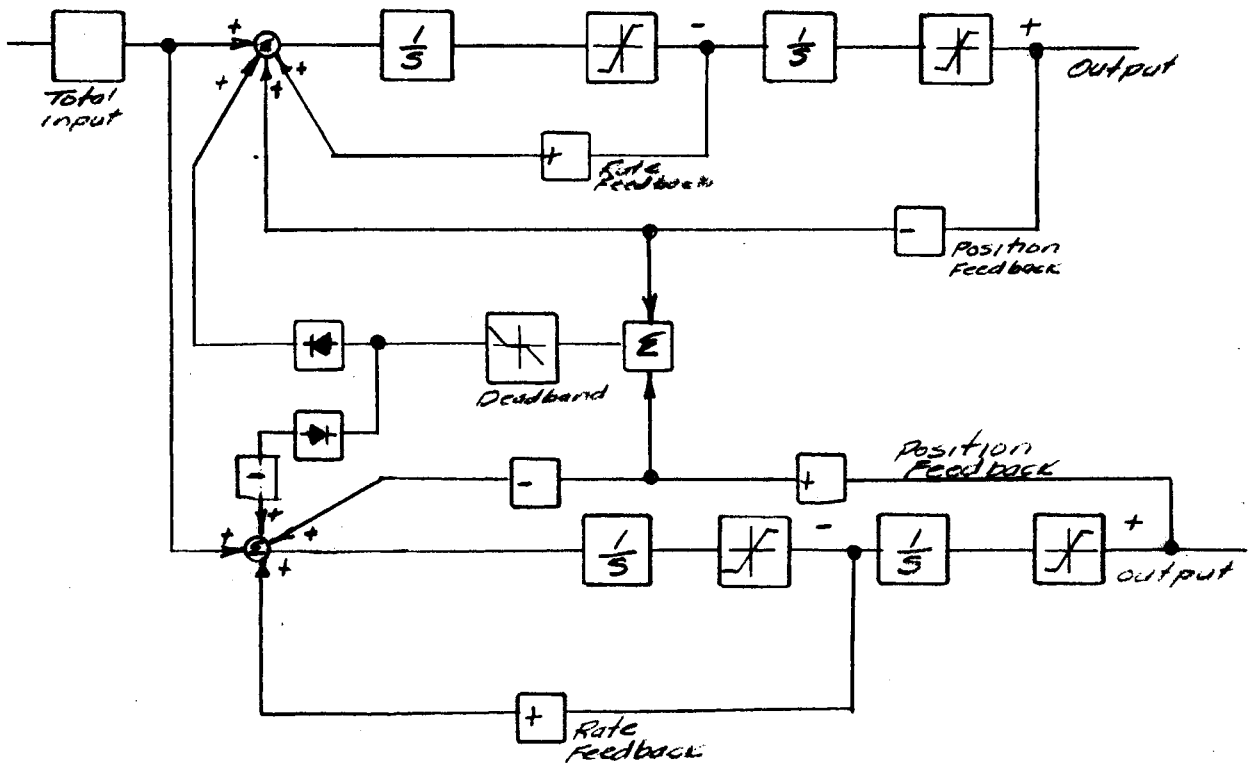
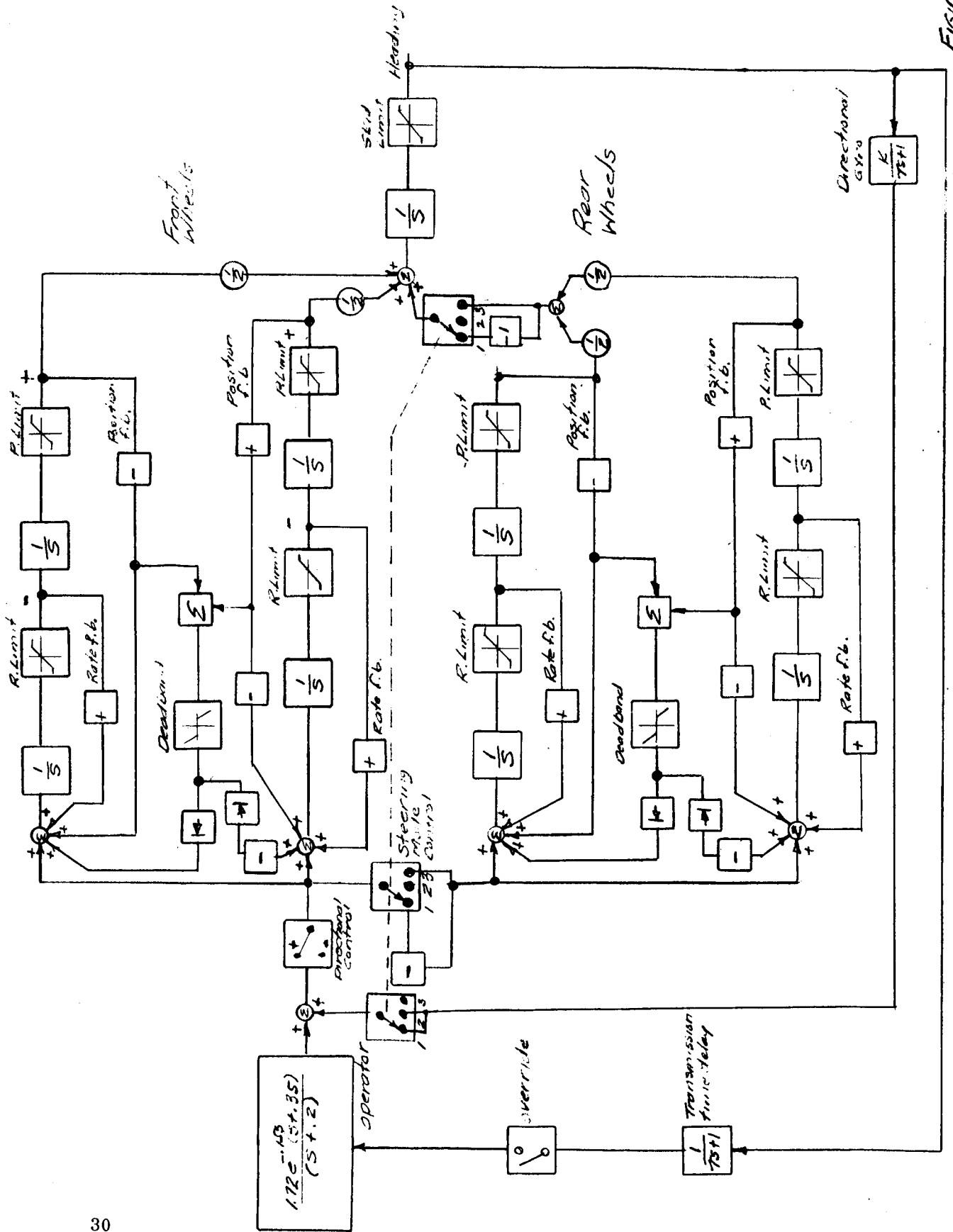


FIGURE 10B CONTROL OF TWO WHEELS (SYNCHRONIZED)

EARTH-TO-LUNAR CONTROL - SYNCHRONIZED ACKERMANN,  
4-WHEEL, AND CRAB STEERING



FIGURE

The concept is a collection of the circuits previously described, with the exception of the selection of the types of steering. Position 1 of the steering mode control switch applies to 4-wheel steering; position 2 applies to Ackermann steering; and position 3 applies to crab steering. It should be noted that Ackermann and 4-wheel steering operate as closed-loop systems with the heading control, while crab steering operates open loop.

#### 4.0 AUTOMATIC CHANGE OF VEHICLE OPERATING LIMITS

Some of the control limits, such as skidding, etc., were discussed in Section 2.4. These limits and those of vehicle overturn primarily limit the speed of the vehicle on the Lunar surface. Vehicle overturn in turn depends (besides speed) on the size of obstacles transversed, the terrain slope, the  $\mu$  of the soil and a combination of these to varied degrees. At first glance it appears desirable to devise automatic circuits in the control systems that would compensate for the conditions of terrain over which the LSV travels. Such changes in limits would compensate speed and wheel angle of the vehicle so that it would be operating within safe conditions. That is, a safe speed set for level ground would be reduced automatically when the vehicle found itself on a slope. Besides the difficulty in implementing such a program; however, it appears impractical. For instance, the results of striking an obstacle with one side of the vehicle have been shown in Reference 1 to produce similar results (measured in seconds of time) as having the vehicle operate on a slope. For another example, pitch plane sensors would record verticle excursions of the LSV (after striking an object) in the same manner as when the vehicle goes up or down a slope. In addition, any sensor operating to limit speed or wheel angle would necessarily take into account the  $\mu$  of the soil. The  $\mu$  could vary in the space of as little as 10 meters with no accurate way of measuring the change. With constant changes in terrain conditions, the task of implementing automatic changes in limits should prove to

be cumbersome. Instead, it appears to be more reasonable initially to set administrative limits of speed and maximum wheel angle below the safe operating limits of the vehicle. In addition pitch, yaw and roll angle information, as well as wheel angle and vehicular speed, should be furnished to any remote operator of the LSV so that the approach to unsafe conditions can be recognized. The set vehicular speeds must be set slow enough to stop the vehicle when an unsafe condition approaches. Speeds of 4Km per hour and wheel angles of  $60^\circ$  (maximum) appear to be acceptable for soil  $\mu$  of 0.4 to 0.5 (Reference 1) and slopes of 0 to  $30^\circ$  for traversing obstacles of up to 0.35 meters high. A reduction in the vehicle speed may be necessary, however, when the Earth-to-Lunar time delay is considered with the control system. It is assumed in this latter case that the control system is employed to by-pass an obstacle.

This study has established a range of motor sizes that can be used to accomplish steering rates in a range of  $3^\circ$  to  $9^\circ$  per second for the wheel angle. Previous work (Reference 1) has shown that practical steering rates lie within this range. Root locus plots have been presented which can be interpreted to indicate dynamic responses of the particular systems for the operating conditions (besides the maximum) for motor speeds, or inputs, lower than that of the design maximum.

The problem of synchronizing the wheel angles of the separately operated wheels used for steering exists. Accordingly, a concept for this operation has been presented.

In each of the above areas studied the final design depends on unknown factors such as the  $\mu$  of the soil and the administrative decision concerning operating speeds of the LSV. Conclusions from this study, therefore, are limited. It is concluded, however, that control systems employing wheel angle control (as opposed to heading control) can be made to be stable with little trouble. Controls systems employing heading control are more sensitive and require computer studies before a final decision is reached. It is recommended that these computer studies be made using the concept diagrams of this report.



## SECTION 6.0

### SYMBOLS

$J$	System Inertia, ounce-inches squared
$K$	Amplifier Gain
$K_S$	Motor Speed Constant, volt-second/radian
$K_T$	Motor Torque Constant, ounce-inches per amp
$K_\theta$	Voltage Feedback Constant, volts/radian
$R$	Motor Armature Resistance, ohms
$T_1$	Steady State Torque Load, ounce-inches
$V_a$	Applied Motor armature voltage, dc volts
$\mathcal{J}$	Damping Ratio
$\gamma$	Coefficient of Friction
$\tau$	Time Constant, seconds
$\psi$	Vehicle heading

## REFERENCES

1. "Apollo Extension System LSV Studies - Mission Command and Control" by Arch W. Meagher and Robert J. Bonham, January 8, 1965 NASA CR-61040
2. "The Human Operator as a Servo Element" by Duane T. McRuer and Ezra S. Krendel, Part I, Frankland Institute Journal May 1959, Part II, Frankland Institute Journal, June 1959.

7.0

Appendix A

Page

- I Steering Motor Size Data -- Typical Control Type
- II Steering Motor Data - 1/8 Horsepower

## STEERING MOTOR SIZE - CALCULATIONS

### General

In order to calculate the motor constants needed for use in the transfer function for servo-analysis, reasonable motor sizes were first calculated from a torque-horsepower relation. This relation was considered from a steady-state view point using the footprint of the Lunar Surface Vehicle (LSV) and the maximum power and torque expected when the vehicle is standing still. A surface  $\gamma$  of 1.0 was used. While there is small likelihood that this combination will be encountered, it must be considered as the worst case.

The actual footprint of the LSV will be elliptical. However, for ease of calculations a rectangular shape was used with a calculated radius of gyration. The difference in footprint shapes is considered in the safety factor of the calculations. Torque and horsepower are considered in the calculations to vary with  $\gamma$ . Figure A1 indicates the pertinent LSV data used in calculating motor sizes.

All motors studied were considered to have fixed or separately excited (shunt) fields. The field strength is not specified except in the armature current, torque and speed constants. Typical small control-type motors were first studied, and it appears that the requirements for steady-state velocity will be satisfied by this type of motor. However, the study (in the text) shows that a larger - or high torque - motor is required for accelerating the system at an acceptable rate.

As a result of these findings, larger motors were studied as well. In all cases for the motor studies the amount of inertia of the vehicle wheel is neglected since it is very small when referred to the armature of the motor. The inertia used for the calculations includes that of the motor, gears and any governor that may be required. The final choice of a motor for steering will be determined by the speed of steering, the allowable heating of the motor, the torque required and a provision for stall current. The small motors shown in this study provide for stall current. The larger motors, however, are for intermittent duty but can be started across the line. They require greater cooling. A compromise must be reached in the final choice of motor.

PERTINENT SPECIFICATIONS OF THE 4 WHEEL LSV  
USED IN THE STEERING MOTOR CALCULATIONS

VEHICLE BODY MASS:	185 Slugs
VEHICLE WHEEL MASS:	4.34 Slugs
VEHICLE WHEEL DIAMETER:	80 inches (2.03 meters)
VEHICLE TIRE WIDTH:	12 inches (0.305 meter)
VEHICLE TIRE CONSTANT:	50 pounds per inch deflection
FOOTPRINT SIZE:	approximate 3.73 ft. <sup>2</sup>

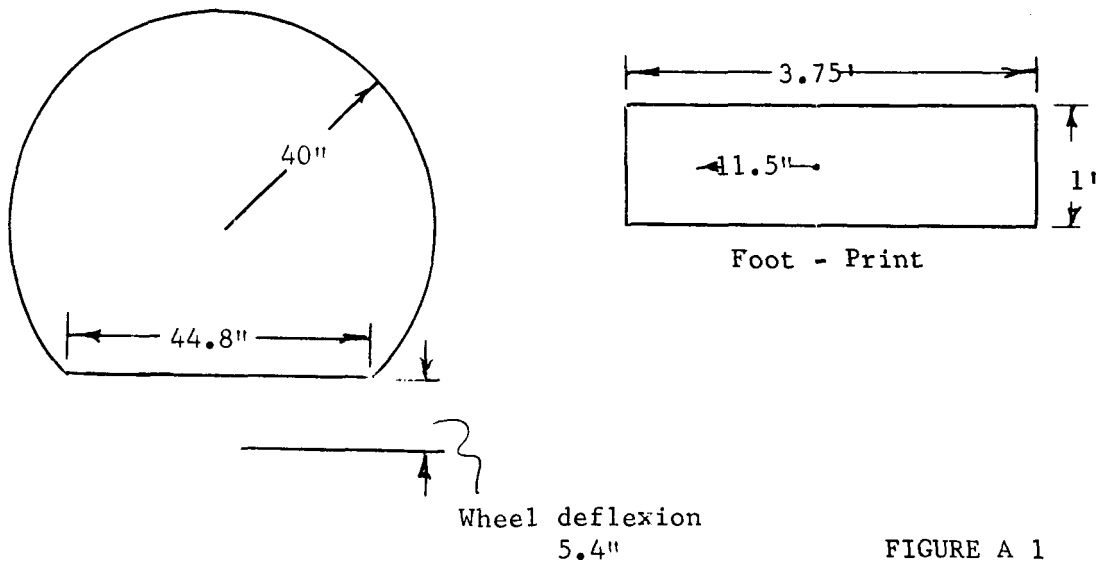


FIGURE A 1

I. STEERING MOTOR SIZE DATA -

TYPICAL CONTROL TYPE

TABLE A I A

APPROXIMATE TORQUE REQUIRED TO  
CHANGE LSV WHEEL ANGLE WITH LSV  
VELOCITY AT ZERO AND WITH VARIOUS  
VALUES OF  $\mu$

	TORQUE REQUIRED OZ - INCHES	TORQUE REQUIRED PLUS 25% SAFETY FACTOR OZ - INCHES
1	3120	3900
0.5	1560	1950
0.2	624	780

TABLE A I B

MOTOR HORSEPOWER REQUIRED FOR VARIOUS  $\mu$  AND STEADY-STATE  
WHEEL-TURN RATES - VEHICLE VELOCITY, 0

Wheel-Turn Rate Degrees/second	$\mu = 1$	$\mu = 0.5$	$\mu = .2$
	Horsepower	Horsepower	Horsepower
3	.031	.016	.006
6	.062	.032	.013
9	.093	.047	.019

T A B L E A I C

SYSTEM DATA FOR USE WITH CONTROL TYPE MOTORS

Wheel-angle Rate Degrees/Sec.	Motor Size Horsepower	Motor Speed R P M	Motor No-Load Speed RPM	System Gear Reduction	Motor Resistance Ohms	Rated Voltage	System inertia at the Motor OZ-In <sup>2</sup>	K <sub>t</sub> oz-in per amp	K <sub>s</sub> volts/rad/Sec
3	$\frac{1}{30}$	3750	5000	7500/1	8	28	1.095	5.58	0.306
6	$\frac{1}{16}$	7500	10,000	7500/1	4	28	1.392	3.23	0.0204
9	$\frac{1}{10}$	7500	8500	5000/1	2	28	1.392	4.0	0.027



TORQUE-SPEED AND TORQUE-CURRENT CURVES  
 (  $\frac{1}{30}$  Horsepower Motor)

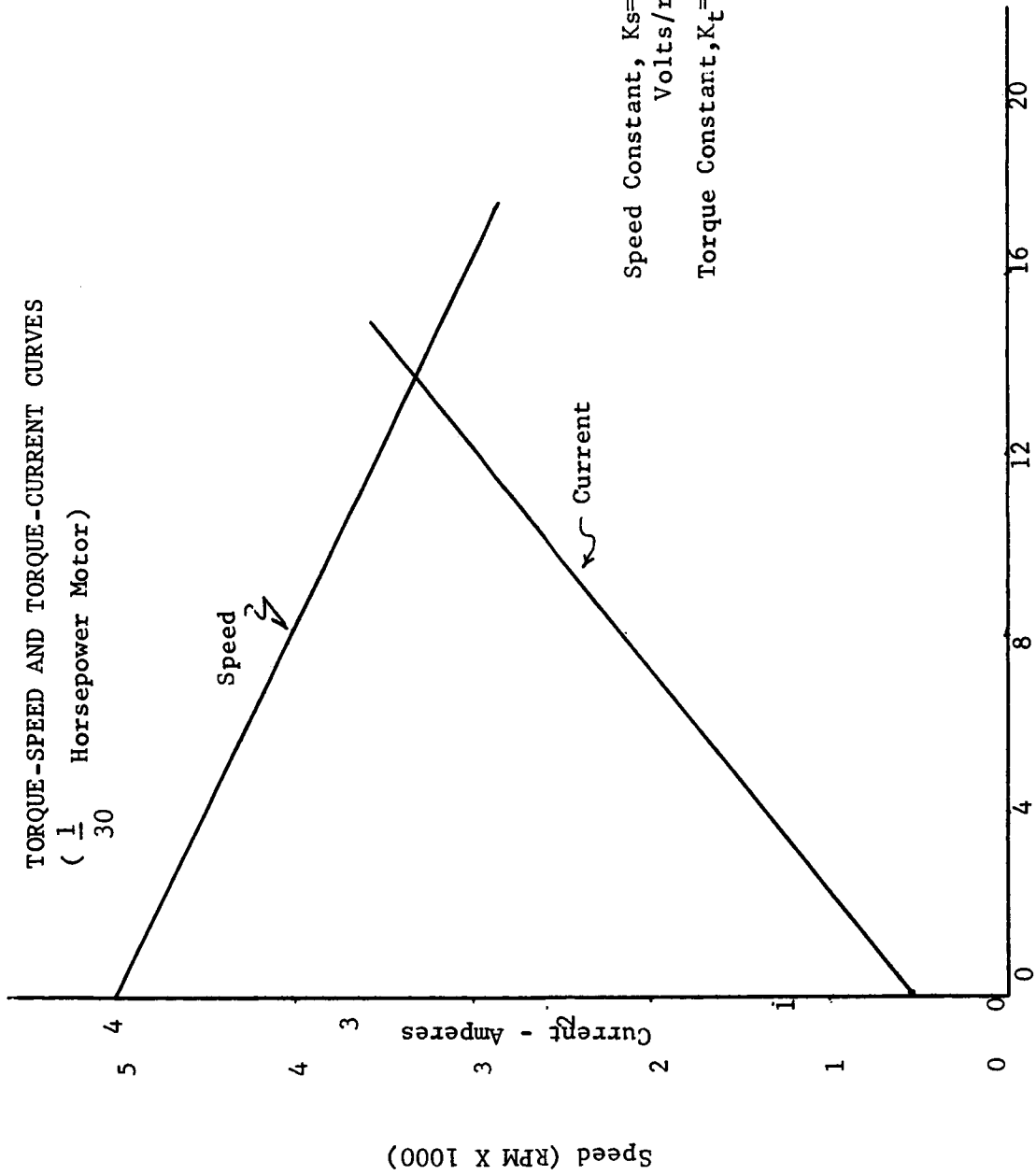
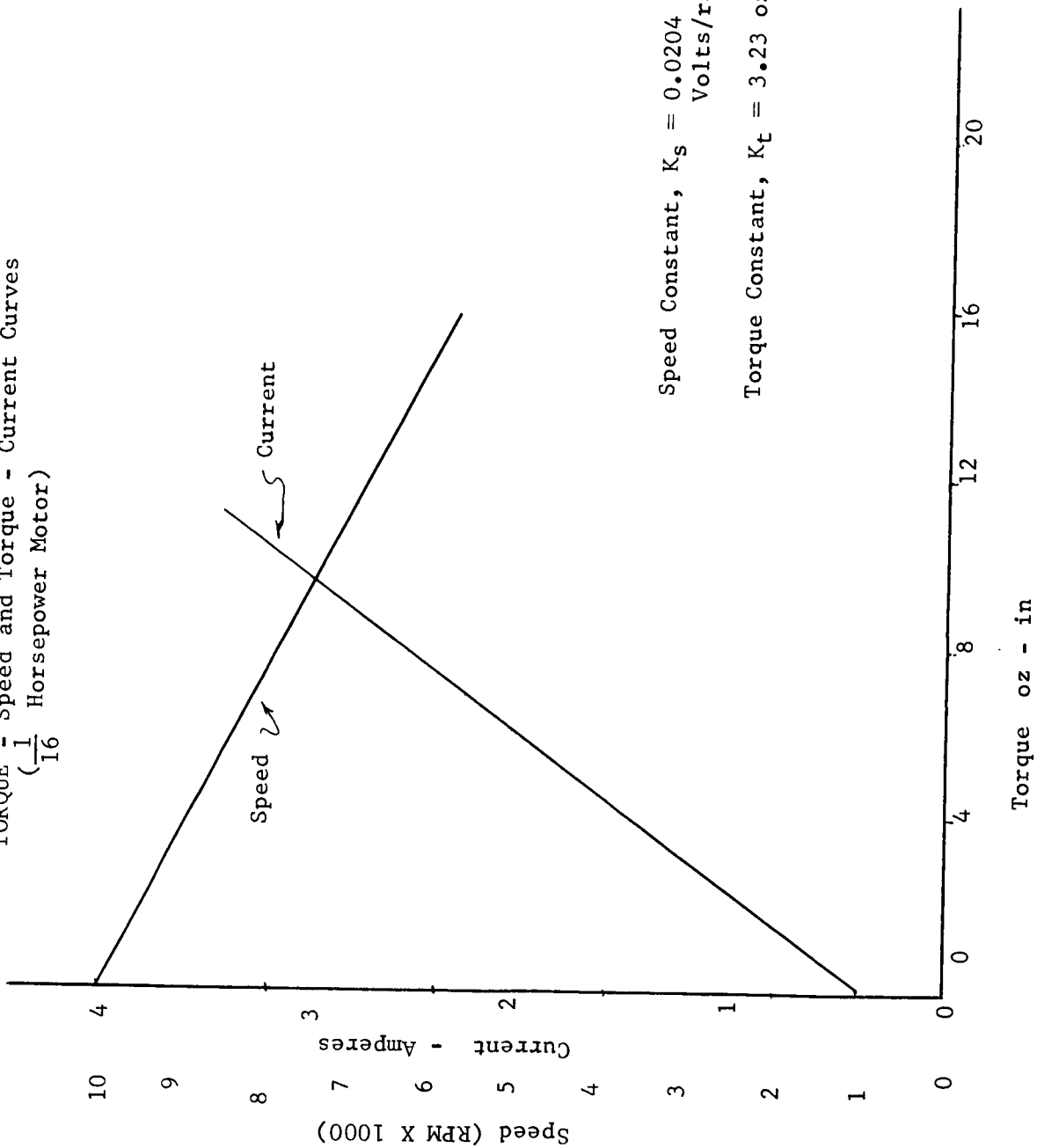


Figure A1A

TORQUE - Speed and Torque - Current Curves  
 ( $\frac{1}{16}$  Horsepower Motor)

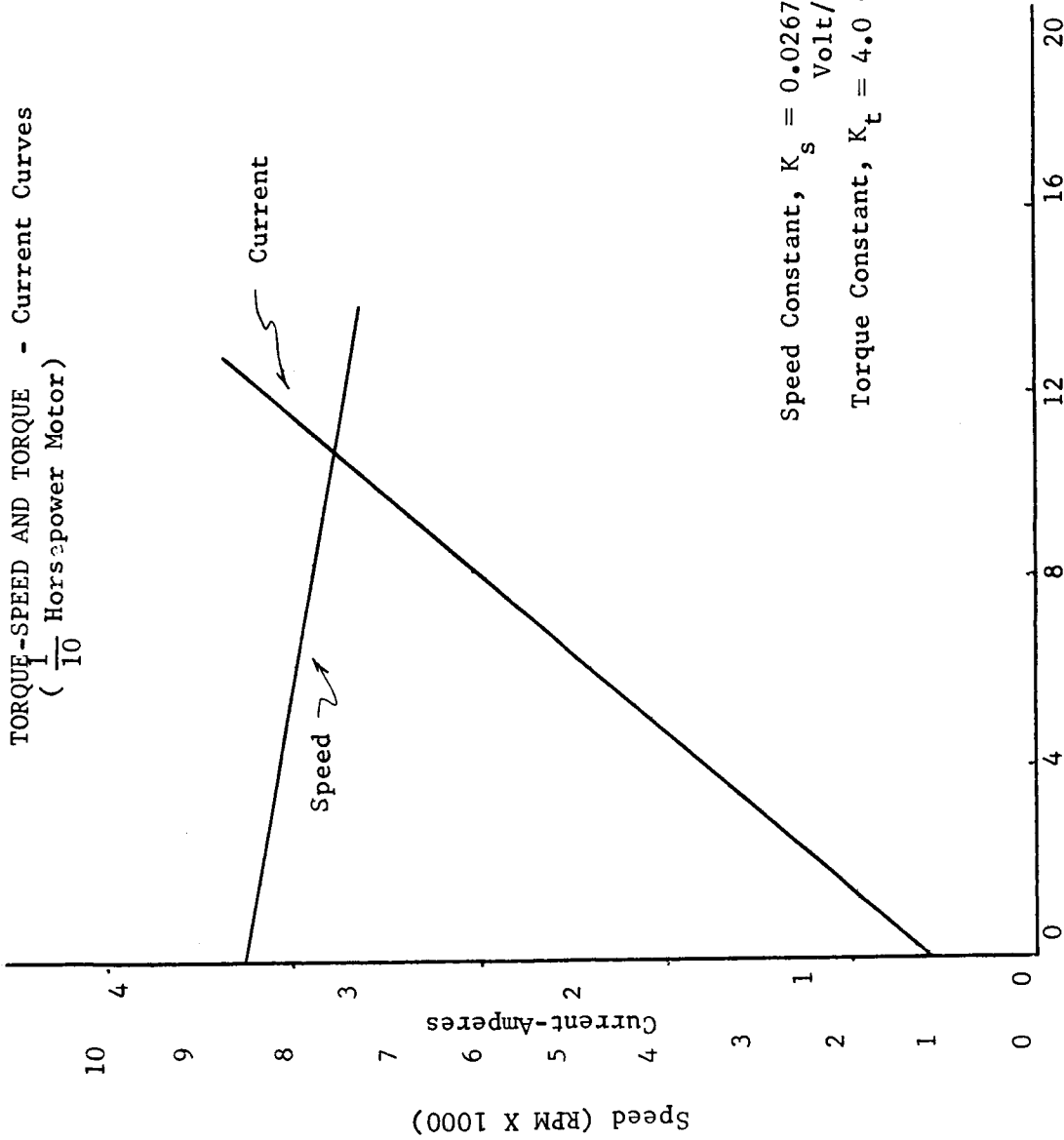


Speed Constant,  $K_s = 0.0204$   
 Volts/rad/sec

Torque Constant,  $K_t = 3.23$  oz-in/Amp

Figure A 2 B

TORQUE-SPEED AND TORQUE - Current Curves  
 (  $\frac{1}{10}$  Horsepower Motor )



Speed Constant,  $K_s = 0.0267$  Volt/rad/sec  
 Torque Constant,  $K_t = 4.0$  Oz-in/Amp

Figure A 2 C

II. STEERING MOTOR DATA -  $\frac{1}{8}$  HORSEPOWER

T A B L E A I I

SYSTEM DATA FOR USE WITH  $\frac{1}{8}$  HORSEPOWER MOTORS

System	Wheel Angle Rate, Degrees per Second	Motor Speed R P M	System Gear Reduction	Motor Resistance Ohms	Rated Voltage	System Inertia at Motor OZ - In <sup>2</sup>	KT OZ-In Per Amp	Ks Volts/Radian/Sec.
A	3	1800	3600/1	2	28	8	108.2	0.148
B	6	3600	3600/1	2	28	8	216.4	0.074
C	9	3600	2400/1	2	28	8	209.0	0.129

DISTRIBUTION

INTERNAL

DIR  
DEP-T  
R-DIR  
R-AERO-DIR  
    -S  
    -SP (23)  
R-ASTR-DIR  
    -A (13)  
R-P&VE-DIR  
    -A  
    -AB (15)  
    -AL (5)  
R-RP-DIR  
    -J (5)  
R-FP-DIR  
R-FP (2)  
R-QUAL-DIR  
    -J (3)  
R-COMP-DIR  
R-ME-DIR  
    -X  
R-TEST-DIR  
    -DIR  
MS-IP  
MS-IPL (8)

Scientific and Technical Information Facility  
P. O. Box 5700  
Bethesda, Maryland  
Attn: NASA Representative (S-AK RKT) (2)

Manned Spacecraft Center  
Houston, Texas  
Mr. Gillespi, MTG  
Miss M. A. Sullivan, RNR  
John M. Eggleston  
C. Corington, ET-23 (1)  
William E. Stanley, ET (2)

Donald Ellston  
Manned Lunar Exploration Investigation  
Astrogeological Branch  
USGS  
Flagstaff, Arizona

Langley Research Center  
Hampton, Virginia  
Mr. R. S. Osborn

EXTERNAL

NASA Headquarters  
MTF Col. T. Evans  
MTF Maj. E. Andrews (2)  
MTF Mr. D. Beattie  
R-1 Dr. James B. Edson  
MTF William Taylor

Kennedy Space Center  
K-DF Mr. von Tiesenhausen

Northrop Space Laboratories  
Huntsville Department  
Space Systems Section (5)